

# An Exceptionally Difficult Binary Quadratic Optimization Problem with Symmetry: a Challenge for The Largest Unsolved QAP Instance Tai256c

Koichi Fujii\*, Sunyoung Kim†, Masakazu Kojima‡, Hans D. Mittelmann§,  
Yuji Shinano¶

October 31, 2022, Revised: October 1, 2024

## Abstract

Tai256c is the largest unsolved quadratic assignment problem (QAP) instance in QAPLIB. It is known that QAP tai256c can be converted into a 256 dimensional binary quadratic optimization problem (BQOP) with a single cardinality constraint which requires the sum of the binary variables to be 92. As the BQOP is much simpler than the original QAP, the conversion increases the possibility to solve the QAP. Solving exactly the BQOP, however, is still very difficult. Indeed, a 1.48% gap remains between the best known upper bound (UB) and lower bound (LB) of the unknown optimal value. This paper shows that the BQOP admits a nontrivial symmetry, a property that makes the BQOP very hard to solve. Despite this difficulty, it is imperative to decrease the gap in order to ultimately solve the BQOP exactly. To effectively improve the LB, we propose an efficient BB method that incorporates a doubly non-negative relaxation, the orbit branching and the isomorphism pruning. With this BB method, a new LB with 1.25% gap is successfully obtained, and computing an LB with 1.0% gap is shown to be still quite difficult.

## 1 Introduction

For a positive integer  $n$ , we let  $N = \{1, \dots, n\}$  represent a set of locations and also a set of facilities. Given  $n \times n$  symmetric matrices  $\mathbf{A} = [a_{ik}]$  and  $\mathbf{B} = [b_{j\ell}]$ , the quadratic assignment problem (QAP) is stated as

$$\zeta^* = \min_{\pi} \sum_{i \in N} \sum_{k \in N}^n a_{ik} b_{\pi(i)\pi(k)}, \quad (1)$$

\*NTT DATA Mathematical Systems Inc., Tokyo 160-00016, Japan (fujii@msi.co.jp).

†Department of Mathematics, Ewha W. University, Seoul, 52 Ewhayeodae-gil, Sudaemoon-gu, Seoul 03760, Korea (skim@ewha.ac.kr). The research was supported by NRF 2021-R1A2C1003810.

‡Department of Industrial and Systems Engineering, Chuo University, Tokyo 192-0393, Japan (kojima@is.titech.ac.jp).

§School of Mathematical and Statistical Sciences, Arizona State University, Tempe, Arizona 85287-1804, U.S.A. (mittelma@asu.edu).

¶Department of Applied Algorithmic Intelligence Methods (A<sup>2</sup>IM), Zuse Institute Berlin, Takustrasse 7,14195 Berlin, Germany (shinano@zib.de).

where  $a_{ik}$  denotes the flow between facilities  $i$  and  $k$ ,  $b_{j\ell} = b_{\ell j}$  the distance between locations  $j$  and  $\ell$ , and  $(\pi(1), \dots, \pi(n))$  a permutation of  $1, \dots, n$  such that  $\pi(i) = j$  if facility  $i$  is assigned to location  $j$ . We assume that the distance  $b_{jj}$  from  $j \in N$  to itself and the flow  $a_{ii}$  from  $i \in N$  to itself are both zero.

The QAP is NP-hard in theory, and solving exactly large scale instances (*e.g.*,  $n \geq 40$ ) is very difficult in practice. To obtain an exact optimal solution, we basically need two types of techniques. The first one is for computing heuristic solutions. Heuristic methods such as tabu search, genetic method and simulated annealing have been developed for the QAP [10, 15, 39, 40]. Those methods often attain near-optimal solutions and occasionally even exact optimal solutions. The exactness is, however, not guaranteed in general. The objective value  $\bar{\zeta}$  obtained by those methods serves as an upper bound (UB) for the unknown optimal value  $\zeta^*$ . The second technique is to provide a lower bound (LB)  $\underline{\zeta}$  for  $\zeta^*$ . If  $\underline{\zeta} = \bar{\zeta}$  holds, then we can conclude that  $\underline{\zeta} = \zeta^* = \bar{\zeta}$ . Various relaxation methods [2, 16, 23, 36, 42] have been proposed for computing LBs. The two techniques mentioned above play essential tools in the branch and bound (BB) method for QAPs [1, 9, 17, 23, 33, 37].

In this paper, we focus on the largest unsolved instance tai256c in QAPLIB [7, 8]. The main purpose of this paper is to investigate the challenge to solve the instance and provide an improved lower bound. Nissofolk et al. [30, 31] showed that tai256c can be converted into a 256-dimensional binary quadratic optimization problem (BQOP) with a single cardinality constraint  $\sum_{i=1}^{256} x_i = 92$ .

$$\zeta^* = \min \left\{ \mathbf{x}^T \mathbf{B} \mathbf{x} : \mathbf{x} \in \{0, 1\}^n \text{ and } \sum_{i=1}^n x_i = 92 \right\}. \quad (2)$$

See Section 2.2. Here each feasible solution  $\pi$  of QAP (1) is converted to a feasible solution  $\mathbf{x}$  of BQOP (2). They further transformed the BQOP (2) to a mixed integer convex quadratic program (MIQP) by the non-diagonal quadratic convex reformulation technique (NDQCR) developed in [20] for the quadratic knapsack problems. An LB = 44,095,032 (1.48% gap with respect to the best known UB 44,759,294) was obtained by applying CPLEX to the resulting MIQP, where CPLEX terminated in almost 8.5 days since the node limit exceeded. In Section 3.2, we reconfirm this difficulty, even when applying the current version of CPLEX (IBM ILOG CPLEX Optimization Studio (version 22.1.1.0) [11]) and Gurobi Optimizer (version 11.0.0) [18], which are expected to be significantly more powerful than the version of CPLEX used over a decade ago, to the MIQP. See also Remark 3.1. This demonstrates that the simple BQOP equivalent to tai256c remains difficult to solve.

We show that BQOP (2) admits a nontrivial symmetry property, inherited from tai256c:

(a) The matrix  $\mathbf{B}$  satisfies

$$\mathbf{x}_\sigma^T \mathbf{B} \mathbf{x}_\sigma = \mathbf{x}^T \mathbf{B} \mathbf{x} \text{ for every } \mathbf{x} \in \{0, 1\}^n \text{ and } \sigma \in \mathcal{G}, \quad (3)$$

where  $\mathcal{G}$  denotes a subgroup of the symmetry group  $\mathcal{S}_n$  on  $\{1, \dots, n\}$  with  $|\mathcal{G}| = 2,048$ .

(b) BQOP (2) has at least 1,024 distinct feasible solutions with the best known UB 44,759,294.

The size of BQOP (2), 256, is not larger than quadratic unconstrained binary problem (QUBO) instances whose optimal solutions are known in the benchmark problem sets [28,

41]. In fact, all QUBO instances with dimension less than 500 in the sets were solved exactly. BQOP (2) involves a single cardinality constraint  $\sum_{i=1}^{256} x_i = 92$  in binary variables  $x_i$  ( $i = 1, \dots, 256$ ), which is expected to make solving BQOP (2) easier in comparison to QUBOs, since it considerably reduces the number of binary feasible solutions. Moreover, it is straightforward to transform BQOP (2) into a QUBO by adding a penalty term  $\lambda(\sum_{i=1}^{256} x_i - 92)^2$  to the objective quadratic form  $\mathbf{x}^T \mathbf{B} \mathbf{x}$  with a sufficiently large  $\lambda > 0$ .

Suppose that a BB method is applied to the BQOP with the best known UB. Then we (implicitly) construct an enumeration tree of its subproblems, where a subproblem is pruned whenever an LB of the subproblem not less than the best known UB of the BQOP (or an optimal solution of the subproblem) is obtained. In general, as the size of a subproblem involving a feasible solution with the best known UB becomes larger, the subproblem is harder to prune. As a result of the feature (b), the BB method cannot terminate in earlier stages since at least 1,024 distinct feasible solutions with the best known UB are distributed over subproblems. Hence, (b) primarily contributes to the difficulty of solving BQOP (2).

To address the difficulty mentioned above in numerically solving BQOP (2) and to compute a new LB better than the known ones, this paper proposes

(c) a BB method to show that the unknown optimal value  $\zeta^*$  is not less than a given  $\hat{\zeta}$ .

Here a *target* LB  $\hat{\zeta}$  is chosen in the interval of the best known LB =  $\underline{\zeta} = 44,095,032$  and UB =  $\bar{\zeta} = 44,759,294$ . We fix  $\hat{\zeta}$  and  $\bar{\zeta}$  before starting the BB method. The BB method terminates immediately after an LB not less than  $\hat{\zeta}$  is obtained. The proposed BB method implements the Lagrangian doubly nonnegative (Lag-DNN) relaxation [21, 22] as a lower bounding procedure for subproblems.

Using this method, we compute a new LB 44,200,000 (1.25% gap) in 39.2 days on a Mac Studio (20 CPU), and provide estimates on the amount of work (the number of subproblems to be solved and the execution time) for larger LBs. If we chose  $\hat{\zeta}$  to be the best known UB =  $\bar{\zeta}$ , then  $\bar{\zeta}$  would be proved to be the optimal value. In this case,  $2.6 \cdot 10^{12}$  days would be required to solve  $6.7 \cdot 10^{16}$  Lag-DNN relaxation subproblems of BQOP (2). This is not an accurate estimate and the execution time certainly depends on a BB method including a lower bounding procedure, a branching rule and the computer used. Nevertheless, it illustrates the extreme difficulty of solving the BQOP.

## Contribution of the paper and existing results

Our first contribution is to show and analyze the nontrivial symmetry property in BQOP (2) induced from tai256c. This BQOP is a simple, low-dimensional, and extremely difficult BQOP instance. As mentioned above, the nontrivial symmetry property (3) makes the BQOP hard to solve.

The second contribution of this paper is a BB method to prove that the unknown optimal value  $\zeta^*$  is not less than a given target LB =  $\bar{\zeta}$ . A BB method with a target LB was originally developed for large scale QAPs, which was successful to obtain improved lower bounds for some of the QAP instances in QAPLIB [7, 8] including sko100a, ..., sko100f, tai80b, tai100b and tai150b (see [27]). The size of QAP tai256c, however, was too large to handle by the original BB method for the QAPs. In the proposed method, we employ three effective techniques: The first one is the Lag-DNN relaxation [21, 22] subproblems of BQOP (2) for the lower bounding procedure. This relaxation is (almost) equivalent to a DNN relaxation

[3, Theorem 2.6], which is known as one of the strongest (numerically tractable) conic relaxations for combinatorial optimization problems [19]. The second one is the standard orbital branching [32, 35] for reducing the size of the enumeration tree of subproblems to be solved. The third one is the isomorphism pruning [24]. This technique works effectively to improve the computational efficiency since the equivalence of some distinct subproblems occurs in the enumeration tree even after the orbital branching is applied. With this BB method, we computed an LB with 1.46% in 0.6 days on a Mac Studio (20 CPU), generating 11,594 nodes. As mentioned, a slightly larger LB with 1.48% gap is the best known one obtained by Nissofolk et al. [31] in 8.5 days when the node limit of CPLEX was reached. Furthermore, we computed a new LB with 1.25% in 39.2 days, generating 1,077,353 nodes, and demonstrated the considerable difficulty in achieving an LB with 1.01% gap. This can also be regarded as an important contribution.

The orbital branching and the isomorphism pruning incorporated into our BB method can completely avoid applying the lower bounding and branching procedures to more than one isomorphic subproblem of BQOP (2). In addition, its size,  $n = 256$ , is small, so we might expect to solve the BQOP relatively easily. However, in Section 4.6, we discuss another significant reason why solving BQOP (2) is extremely difficult compared to popular benchmark QUBOs with size  $n \leq 256$ .

Exploiting symmetries of QAPs in their SDP relaxation was discussed in [12, 13, 34] (also [6] in their DNN relaxation). However, those results are not relevant to the subsequent discussion of this paper.

## Outline of the paper

In Section 2, we introduce key components that will be utilized in the subsequent sections, including the conversion of QAP (1) into BQOP (2) satisfying the symmetry property (3), the Lag-DNN relaxation and the Newton-bracketing (NB) method for solving the relaxation. In Section 3, we present computational results using DABS (Diverse Adaptive Bulk Search, a genetic algorithm-based search algorithm) [29], Gurobi and CPLEX. We show that state-of-the-art BQOP solver Gurobi could not improve the known LB  $\zeta$ , demonstrating the difficulty of the problem. In Section 4, we describe the BB method (c) in detail and report numerical results. We conclude the paper in Section 5.

## 2 Preliminaries

### 2.1 Notation and symbols

Let  $N = \{1, \dots, n\}$ . We are mainly concerned with the BQOP (2) induced from tai256c. In that case,  $n = 256$ . Let  $\mathbb{R}^n$  denotes the  $n$ -dimensional Euclidean space of column vectors  $\mathbf{x} = (x_1, \dots, x_n)$ , and  $\mathbb{R}_+^n$  its nonnegative orthant  $\{\mathbf{x} \in \mathbb{R}^n : x_i \geq 0 \ (i \in N)\}$ . For  $\mathbf{x} \in \mathbb{R}^n$ ,  $\mathbf{x}^T$  is the transpose of  $\mathbf{x}$ . For each permutation  $\sigma$  of  $N$  and each  $\mathbf{x} \in \{0, 1\}^n \subset \mathbb{R}_+^n$ ,  $\mathbf{x}_\sigma$  denotes  $\mathbf{x}' \in \{0, 1\}^n$  such that  $x'_j = x_{\sigma(i)}$  ( $i \in N$ ).  $\mathbb{R}^{m \times n}$  denotes the linear space of  $m \times n$  matrices.  $\mathbb{S}^n$  denotes the linear space of  $n \times n$  symmetric matrices with the inner product  $\mathbf{A} \bullet \mathbf{B} = \sum_{i \in N} \sum_{j \in N} A_{ij} B_{ij}$  for  $\mathbf{A}, \mathbf{B} \in \mathbb{S}^n$ ,  $\mathbb{S}_+^n$  the convex cone of positive semidefinite matrices in  $\mathbb{S}^n$ , and  $\mathbb{N}^n$  the convex cone of matrices with nonnegative elements in  $\mathbb{S}^n$ .

## 2.2 Conversion from tai256c to BQOP (2)

QAP (1) can be rewritten with an  $n \times n$  matrix variable  $\mathbf{X}$  as a quadratic optimization problem:

$$\zeta^* = \inf \{(\mathbf{A}\mathbf{X}\mathbf{B}) \bullet \mathbf{X} : \mathbf{X} \in \Pi\}, \quad (4)$$

where  $\Pi$  denotes the set of  $n \times n$  permutation matrix. We note that each feasible solution  $\pi$  of QAP (1), which is a permutation of  $N$ , corresponds to an  $\mathbf{X} \in \Pi$  such that  $X_{ij} = 1$  iff  $\pi(i) = j$  for every  $(i, j) \in N \times N$ . In case of tai256c,  $n = 256$  and  $\mathbf{A}$  can be represented as  $\mathbf{A} = \mathbf{f}\mathbf{f}^T$  for  $\mathbf{f} = \begin{pmatrix} \mathbf{e} \\ \mathbf{0} \end{pmatrix}$ , where  $\mathbf{e}$  denotes the 92-dimensional column vector of 1's. Hence, the objective function  $(\mathbf{A}\mathbf{X}\mathbf{B}) \bullet \mathbf{X}$  of QAP (4) can be rewritten as

$$(\mathbf{A}\mathbf{X}\mathbf{B}) \bullet \mathbf{X} = (\mathbf{f}\mathbf{f}^T\mathbf{X}\mathbf{B}) \bullet \mathbf{X}^T = (\mathbf{X}^T\mathbf{f})^T\mathbf{B}(\mathbf{X}^T\mathbf{f}).$$

We then see that  $\mathbf{x} = \mathbf{X}^T\mathbf{f} \in \{0, 1\}^n$  and  $\sum_{i \in N} x_i = 92$  for every  $\mathbf{X} \in \Pi$ . Conversely, if  $\mathbf{x} \in \{0, 1\}^n$  and  $\sum_{i \in N} x_i = 92$ , then  $\mathbf{x} = \mathbf{X}^T\mathbf{f}$  for some  $\mathbf{X} \in \Pi$ . Therefore, QAP (4) (hence QAP (1)) is equivalent to BQOP (2).

**Remark 2.1.** The conversion from tai256c to BQOP (2) can also be carried out by the clone shrinking method in [14, Theorem1].

## 2.3 Symmetry of the matrix $\mathbf{B}$

We computed  $\mathcal{G}$  by a simple implicit enumeration of permutations  $\sigma$  satisfying (3), and found:

- $|\mathcal{G}| = 2,048$
- The best known feasible solution  $\mathbf{x}^*$  of BQOP (2) with the objective value, which is equal to the best known UB 44,759,294 for tai256c, is further expanded to the set of feasible solutions  $\{(\mathbf{x}^*)_\sigma : \sigma \in \mathcal{G}\}$  with the common objective value, where  $|\{(\mathbf{x}^*)_\sigma : \sigma \in \mathcal{G}\}| = 1024$ ;  $(\mathbf{x}^*)_\sigma = (\mathbf{x}^*)_{\sigma'}$  can occur for distinct  $\sigma \in \mathcal{G}$  and  $\sigma' \in \mathcal{G}$ .

Computing the group  $\mathcal{G}$  of permutations can also be carried out with the software called Nauty [25]. The symmetry of  $\mathbf{B}$  is utilized in orbital branching (Section 4.2) and eliminating equivalent subproblems (Section 4.5) which are implemented in the BB method for solving BQOP (2).

## 2.4 A Lagrangian doubly nonnegative (Lag-DNN) relaxation of a linearly constrained QOP in binary variables

We briefly present a Lag-DNN relaxation, which was originally proposed in [21] combined with the the bisection-projection (BP) method for computing LBs of linearly constrained QOPs in binary variables. More recently, the BP method was further enhanced to the Newton-bracketing (NB) method [22] by replacing the bisection method with the Newton method for the largest zero of a continuously differentiable convex function  $g : \mathbb{R} \rightarrow [0, \infty)$  (see Figure 1 and Section 2.5) In our proposed BB method, the NB method is used for

computing LBs of BQOP (2). BQOP (2) as well as its subproblem BQOP( $I_0, I_1$ ) presented in Section 4.1, are special cases of a linearly constrained QOP in binary variables.

$$\zeta = \inf \{ \mathbf{u}^T \mathbf{C} \mathbf{u} : \mathbf{u} \in \{0, 1\}^n, \mathbf{F} \mathbf{u} - \mathbf{b} s = \mathbf{0}, s = 1 \}, \quad (5)$$

where  $\mathbf{C} \in \mathbb{S}^n$ ,  $\mathbf{F} \in \mathbb{R}^{m \times n}$  and  $\mathbf{b} \in \mathbb{R}^m$ .

BQOP (5) is rewritten to strengthen the DNN relaxation by introducing slack variable vector  $\mathbf{v} \in \{0, 1\}^n$  for  $\mathbf{u} \in \{0, 1\}^n$ :

$$\zeta = \inf \left\{ \mathbf{u}^T \mathbf{C} \mathbf{u} : \begin{array}{l} (\mathbf{u}, \mathbf{v}, s) \geq \mathbf{0}, (u_j + v_j - s)^2 = 0 \ (j \in N), \\ u_j v_j = 0 \ (j \in N), (\mathbf{F} \mathbf{u} - \mathbf{b} s)^T (\mathbf{F} \mathbf{u} - \mathbf{b} s) = 0, s^2 = 1 \end{array} \right\} \quad (6)$$

Introducing a penalty function (or a Lagrange function)

$$\begin{aligned} L(\mathbf{u}, \mathbf{v}, s, \lambda) &= \mathbf{u}^T \mathbf{C} \mathbf{u} + \lambda \left( \sum_{j \in N} (u_j + v_j - s)^2 + \sum_{j \in N} u_j v_j \right. \\ &\quad \left. + (\mathbf{F} \mathbf{u} - \mathbf{b} s)^T (\mathbf{F} \mathbf{u} - \mathbf{b} s) \right) \text{ for every } (\mathbf{u}, \mathbf{v}, s, \lambda) \geq \mathbf{0}, \end{aligned}$$

we consider a simple QOP

$$\zeta(\lambda) = \inf \{ L(\mathbf{u}, \mathbf{v}, s, \lambda) : (\mathbf{u}, \mathbf{v}, s) \geq \mathbf{0}, s^2 = 1 \},$$

where  $\lambda \geq 0$  denotes a penalty parameter (or a Lagrangian multiplier). We can prove that  $\zeta(\lambda)$  converges to  $\zeta$  as  $\lambda \rightarrow \infty$ . See [21, Lemma 3]. The sum  $\mathbf{u}^T \mathbf{C} \mathbf{u} + \sum_{j \in N} u_j v_j + (\mathbf{F} \mathbf{u} - \mathbf{b} s)^T (\mathbf{F} \mathbf{u} - \mathbf{b} s)$ , which correspond the sum of the first, third and fourth term of  $L(\mathbf{u}, \mathbf{v}, s, \lambda)$  and form a quadratic form in  $(\mathbf{u}, \mathbf{v}, s) \in \mathbb{R}^{2n+1}$ , can be represented as  $\mathbf{Q}^1 \bullet \left( \begin{pmatrix} \mathbf{u} \\ \mathbf{v} \\ s \end{pmatrix} \begin{pmatrix} \mathbf{u} \\ \mathbf{v} \\ s \end{pmatrix}^T \right)$  for some  $\mathbf{Q}^1 \in \mathbb{S}^{2n+1}$ . Additionally, the second term  $\lambda (\sum_{j \in N} (u_j + v_j - s)^2)$  can be written as  $\lambda \mathbf{Q}^2 \bullet \left( \begin{pmatrix} \mathbf{u} \\ \mathbf{v} \\ s \end{pmatrix} \begin{pmatrix} \mathbf{u} \\ \mathbf{v} \\ s \end{pmatrix}^T \right)$  for some  $\mathbf{Q}^2 \in \mathbb{S}_+^{2n+1}$  since it is a positive semidefinite quadratic form in  $(\mathbf{u}, \mathbf{v}, s) \in \mathbb{R}^{2n+1}$  for each fixed  $\lambda \geq 0$  and linear in  $\lambda \geq 0$  for each fixed  $(\mathbf{u}, \mathbf{v}, s) \in \mathbb{R}^{2n+1}$ . Thus, letting  $\mathbf{Q}_\lambda = (\mathbf{Q}^1 + \lambda \mathbf{Q}^2)$ , we have

$$L(\mathbf{u}, \mathbf{v}, s, \lambda) = \mathbf{Q}_\lambda \bullet \left( \begin{pmatrix} \mathbf{u} \\ \mathbf{v} \\ s \end{pmatrix} \begin{pmatrix} \mathbf{u} \\ \mathbf{v} \\ s \end{pmatrix}^T \right) \text{ for every } (\mathbf{u}, \mathbf{v}, s, \lambda) \geq \mathbf{0},$$

and

$$\zeta(\lambda) = \inf \left\{ \mathbf{Q}_\lambda \bullet \left( \begin{pmatrix} \mathbf{u} \\ \mathbf{v} \\ s \end{pmatrix} \begin{pmatrix} \mathbf{u} \\ \mathbf{v} \\ s \end{pmatrix}^T \right) : \begin{array}{l} (\mathbf{u}, \mathbf{v}, s) \geq \mathbf{0}, \\ \mathbf{H} \bullet \left( \begin{pmatrix} \mathbf{u} \\ \mathbf{v} \\ s \end{pmatrix} \begin{pmatrix} \mathbf{u} \\ \mathbf{v} \\ s \end{pmatrix}^T \right) = 1 \end{array} \right\},$$

where  $\mathbf{H}$  denotes the  $(2n+1) \times (2n+1)$  matrix with elements  $H_{ij} = 0$  ( $(i, j) \neq (2n+1, 2n+1)$ ) and  $H_{2n+1, 2n+1} = 1$ . By replacing  $\begin{pmatrix} \mathbf{u} \\ \mathbf{v} \\ s \end{pmatrix} \begin{pmatrix} \mathbf{u} \\ \mathbf{v} \\ s \end{pmatrix}^T$  by a matrix variable  $\mathbf{W} \in \mathbb{S}^{2n+1}$ , we obtain a Lag-DNN relaxation of BQOP (5).

$$\eta(\lambda) = \inf \{ \mathbf{Q}_\lambda \bullet \mathbf{W} : \mathbf{W} \in \mathbb{K}, \mathbf{H} \bullet \mathbf{W} = 1 \}, \quad (7)$$

where  $\mathbb{K} = \mathbb{S}_+^{2n+1} \cap \mathbb{N}^{2n+1}$  denotes the  $(2n+1)$ -dimensional DNN cone. We note that a DNN relaxation of BQOP (6) can be written as

$$\eta = \inf \{ \mathbf{Q}^1 \bullet \mathbf{W} : \mathbf{W} \in \mathbb{K}, \mathbf{Q}^2 \bullet \mathbf{W} = 0, \mathbf{H} \bullet \mathbf{W} = 1 \}.$$

The Lag-DNN relaxation (7) is almost as strong as the DNN relaxation above in the sense that  $\eta \geq \eta(\lambda)$  converges monotonically to  $\eta$  as  $\lambda \rightarrow \infty$ . See [3, Theorem 2.6]. In Section 4, which presents numerical results for the BB method applied to BQOP (2), a value of  $\lambda = 10^8 / \|\mathbf{Q}^1\|$  is used.

## 2.5 The Newton-bracketing (NB) Method [3, 22]

Given  $b_0 > \eta(\lambda)$ , the NB Method applied to (7) generates a sequence of intervals  $[a_k, b_k]$  ( $k = 0, 1, \dots$ ) which converges to  $\eta(\lambda)$  monotonically. In this section, we briefly present how the sequence is generated. For more details, we refer to [4, Section 3], [3, Section 4] and [22]. Throughout this section,  $\lambda > 0$  is fixed. The dual of DNN problem (7) can be written as

$$y^* = \sup \{ y : \mathbf{Q}_\lambda - \mathbf{H}y = \mathbf{Y} \in \mathbb{K}^* \}, \quad (8)$$

where  $\mathbb{K}^* = \mathbb{S}_+^{2n+1} + \mathbb{N}^{2n+1}$  (the dual of the  $(2n+1)$ -dim. DNN cone  $\mathbb{K} = \mathbb{S}_+^{2n+1} \cap \mathbb{N}^{2n+1}$ ). By strong duality (see [3, Lemma 2.3]),  $y^* = \eta(\lambda)$  holds. Define the function  $g : \mathbb{R} \rightarrow \mathbb{R}$  as

$$g(y) = \inf \{ \|\mathbf{Q}_\lambda - \mathbf{H}y - \mathbf{Y}\| : \mathbf{Y} \in \mathbb{K}^* \} \text{ for every } y \in \mathbb{R},$$

which satisfies the following properties:

- (i)  $g(y) \geq 0$  for every  $y \in \mathbb{R}$ .
- (ii)  $\mathbf{Y} = \mathbf{Q}_\lambda - \mathbf{H}y \in \mathbb{K}^*$  (*i.e.*,  $(y, \mathbf{Y})$  is a feasible solution of (8)) if and only if  $g(y) = 0$ .
- (iii)  $g(y^*) = 0$ .
- (iv)  $g(y) = 0$  if  $y \leq y^*$  (since  $\mathbf{H} \in \mathbb{K}^*$ ).

Hence,  $y^*$  corresponds to the maximum zero of  $g$ . Furthermore,  $g : (y^*, \infty) \rightarrow \mathbb{R}$  is convex and continuously differentiable ([3, Lemma 4.1]). Therefore, we can generate a sequence  $(y_k)_{k=0}^\infty$  converging monotonically to  $\eta(\lambda)$  by applying the Newton method with a given initial point  $y_0 > y^*$ . See Figure 1. The function value  $g(y)$  and the derivative  $g'(y)$  at  $y = y_k > y^*$  is not given explicitly but can be computed by the accelerated proximal gradient (APG) method [5]. This method also computes  $(\mathbf{Y}_k^1, \mathbf{Y}_k^2) \in \mathbb{S}_+^{2n+1} \times \mathbb{N}^{2n+1}$  which (approximately) satisfies  $\mathbf{Q}_\lambda - \mathbf{H}y_k = \mathbf{Y}_k^1 + \mathbf{Y}_k^2$ . and  $\mathbf{Y}_k^1 \in \mathbb{S}_+^{2n+1}$ . We obtain  $a_k \leq y^*$  by letting

$$a_k = y_k + (n+1) \min\{0, \text{the minimum eigenvalue of } \mathbf{Y}_k^1\}.$$

See [4, Lemma 3.1]. In each iteration of the NB method, most of its execution time is consumed to evaluate  $g(y_k)$ ,  $g'(y_k)$ ,  $\mathbf{Y}_k^1$  and  $\mathbf{Y}_k^2$  by the APG method.

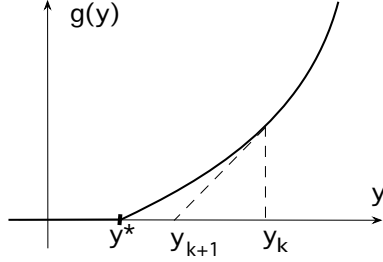


Figure 1: The convex function  $g : \mathbb{R} \rightarrow \mathbb{R}_+$  and the NB method.

### 3 Numerical experiments using the QUBO solver and MIQP solvers

#### 3.1 Solving BQOP (2) with QUBO and MIQP Solvers

We report computational results obtained by DABS (Diverse Adaptive Bulk Search), a genetic algorithm-based search algorithm for QUBO [29], and a general BQOP solver Gurobi Optimizer (version 11.0.0) [18], for BQOP (2). Numerical experiments were conducted on Intel(R) Xeon(R) Gold 6246 (3.30 GHz) processors using 48 threads with 1.5TB of RAM.

BQOP (2) with a single cardinality constraint  $\sum_{i=1}^n x_i = 92$  can be transformed to a simple QUBO by adding the penalty term  $\lambda(\sum_{i=1}^n x_i - 92)^2$  to the objective function  $\mathbf{x}^T \mathbf{Q} \mathbf{x}$  and removing the constraint, where  $\lambda > 0$  is a penalty parameter. We applied DABS to the resulting QUBO with  $\lambda = 10^7$ . DABS attained a feasible solution with the objective value of 44,759,294, which coincides with the best known upper bound [7, 8] for tai256c, within a few seconds. Moreover, the feasible solution computed is contained in the 1,024 known ones with the same objective value of 44,759,294 (see Section 2.3).

We also applied Gurobi to BQOP (2). Gurobi is state-of-the-art as a solver for general BQOPs. In a benchmark project conducted by Mittelman [26], several solvers are tested for BQOPs. The results there indicate that Gurobi is the fastest in solving those BQOPs. Gurobi has been enhanced as a BQOP solver, and its performance and efficiency in this specific area have been constantly improved. In Section 4.2, we will see from the symmetry of  $\mathbf{B}$  that BQOP (2) has an optimal solution  $\mathbf{x}$  with  $x_1 = 1$ . When Gurobi was applied to BQOP (2) with  $x_1$  fixed to 1, the internal log indicated that 255 variables were grouped into 44 orbits, with one of the orbits consisting of only a single variable. As we will see in Table 4.2 (Section 4), this coincides with the symmetry detected by our method.

To experiment with Gurobi, some parameters were needed to be decided, in particular `MIPFocus`, and `PreQLinearize`. The parameter `MIPFocus` controls the solution strategy of branch-and-bound. We chose `MIPFocus=3` which focuses on computing the LB. The parameter `PreQLinearize` controls presolving for BQOPs. More precisely, the parameter `PreQLinearize=0` adds neither any variables nor constraints, but it performs adjustments on quadratic objective functions to make them positive semidefinite. The parameter values `PreQLinearize=1` and `PreQLinearize=2` attempt to linearize quadratic constraints or a quadratic objective, replacing quadratic terms with linear terms with additional variables and linear constraints.



In the first step, we examined the value of `PreQLinearize` by comparing the LB obtained at the root node. `PreQLinearize=0` provided the LB 41,172,797, `PreQLinearize=1` the LB 10,759,778, and `PreQLinearize=2` the LB 3,987,504. As the best LB 41,172,797 among the three was obtained by `PreQLinearize=0`, we adopted this setting for our experiments.

In the second step, we examined 1,024 potentially best solutions generated by the symmetry of BQOP (2). We determine the best initial solution among them by executing branch-and-bound with a time limit of 1 hour and comparing the LBs.

In the final step, we executed branch-and-bound with `MIPFocus=3`, `PreQLinearize=0` and the initial solution chosen in the second step. We had to set a time limit of 60,000 seconds due to limitations in computational resources. We finally obtained an LB of 41,669,052 using Gurobi, which generated 12,518,148 nodes.

The LB 41,669,052 obtained is significantly lower than the LBs we will present in Section 4. This suggests that, despite its rapid improvement in solving BQOP problems, the state-of-the-art general BQOP solver is still considerably less effective in solving BQOP (2) or improving its LB.

There are two primary factors for Gurobi’s poor performance in solving BQOP (2). Recall that the LB 41,172,797 (8.01% gap) was obtained at the root node problem. We applied the Lag-DNN relaxation to the same problem and computed an LB 43,881,304 (1.96% gap) of the problem by the NB method in less than 10 minutes. This shows that the LB procedure incorporated in Gurobi is much weaker than the Lag-DNN relaxation. Another noteworthy factor contributing to Gurobi’s poor performance is its inability to fully utilize the symmetry property of BQOP (2). This also played a role in the generation of a huge number of nodes, reaching 12,518,148, by Gurobi to compute the LB 41,669,052 (6.90%) which is still much smaller than the LB 43,881,304 (1.96%) of the root node computed by the Lag-DNN relaxation. This sharply contrasts with our improved BB method, which generated 1,077,353 nodes to compute the LB 44,200,000 (1.25%) in 39.2 days. See Section 4.5.

### 3.2 NDQCR method

We also tested the NDQCR method [30, 31] with Gurobi and IBM ILOG CPLEX Optimization Studio (version 22.1.1.0). Numerical experiments were conducted on Intel(R) Xeon(R) Gold 6230 (2.10 GHz) processors using 32 threads with 385 GB of RAM. The NDQCR involves the following three steps to construct an MIQP:

1. Add a set of quadratic inequalities to BQOP (2) by applying the reformulation-linearization technique (RLT) [38].
2. Solve the primal-dual pair of SDP relaxations of the resulting quadratically constrained quadratic program (QCQP).
3. Formulate an MIQP effectively utilizing the information from the optimal solution of the dual SDP relaxation problem.

We formulated the dual problem of the SDP relaxation of BQOP(2), and solved it using MATLAB R2023b in 212.53 seconds. We then solved the MIQP, which was strengthened by utilizing the optimal solution of the dual SDP relaxation, with CPLEX and Gurobi. For both solvers, we conducted runs for 24 hours and 9 days, utilizing 32 threads. With CPLEX, the LB 43,928,939 was obtained after 24 hours and the LB 43,950,303 after 9 days, reaching

a total of 62,563,872 nodes. With Gurobi, an LB 44,011,626 was obtained after 24 hours and an LB 44,035,000 after 4.97 days, exhausting 385 GB of memory and reaching a total of 139,859,181 nodes. The NDQCR method can obtain the LB 43,848,767 (2.03% gap) at the root node, which is competitive with the NB method. However, the LB increases only gradually, causing the branch-and-bound tree to expand rapidly. The NDQCR method is expected to require increasingly longer CPU time and encounter difficulties with the rapid explosion of nodes needed to compute higher quality LBs.

**Remark 3.1.** The technical details of the NDQCR method tested above are different from the original NDQCR method proposed in [30, 31] because the code of the original NDQCR method was not available from the authors. We tried to incorporate the basic ideas 1, 2 and 3 mentioned above to simulate the original NDQCR method. Although the NDQCR method tested did not attain the same performance as the original one, it encountered the same difficulties with the rapid explosion of nodes.

## 4 A branch and bound method for a given target lower bound

The optimal value  $\zeta^*$  of BQOP (2) remains unknown, with an LB  $\underline{\zeta} = 44,095,032 \leq \zeta^* \leq$  a UB  $\bar{\zeta} = 44,759,294$  exhibiting a 1.48% gap between them. We need to improve the UB and/or the LB to compute the optimal value  $\zeta^*$ . To improve the LB, we propose a BB method. For the lower bounding procedure, we use the Lag-DNN relaxation of a subproblem and the NB method for computing its optimal value which serves as an LB of the subproblem. See Sections 2.4 and 2.5 for the Lag-DNN relaxation and the NB method, respectively. Any upper bounding procedure is not incorporated. Before the start of the BB method, a target LB,  $\hat{\zeta}$ , is first set such that  $\underline{\zeta} = 44,095,032 < \hat{\zeta} \leq \bar{\zeta} = 44,759,294$ . A target LB,  $\hat{\zeta}$ , is the desired value to obtain. Ideally, we want to set  $\hat{\zeta} = \bar{\zeta}$  to confirm whether  $\bar{\zeta}$  is the optimal value. But such a setting may be too ambitious, and requires much stronger computing power than the machine currently used. As a larger  $\hat{\zeta}$  is set, the computational cost rapidly increases as we will see in Section 4.3.

We describe a class of subproblems of BQOP (2) which appear in the enumeration tree generated by the BB method in Section 4.1, and the orbital branching, the branching procedure used in the BB method in Section 4.2. Before presenting numerical results on the BB method in Section 4.4, we provide a preliminary estimate in Table 2 for the amount of work (the number of nodes to generate and execution time) to attain given target LBs by the BB method in Section 4.3. We note that the preliminary estimate was obtained using the orbital branching, without employing the isomorphism pruning described in Section 4.5. Based on this estimation, we choose appropriate LBs as targets for the numerical experiment on the BB method whose results are reported in Section 4.4. In Section 4.5, we present the isomorphism pruning [24] to improve the performance of the BB method. Our numerical results on the original and improved BB methods, which are summarized in Tables 3 and 4, respectively, demonstrate that employing the isomorphism pruning is expected to halve the computational effort compared to using —redthe orbital branching alone. A new LB  $\hat{\zeta} = 44,200,000$  (1.25% gap) is also attained by the improved BB method in 39.2 days.

## 4.1 A class of subproblems of BQOP (2)

Let

$$\mathcal{S} = \left\{ (I_0, I_1, F) : \begin{array}{l} \text{a partition of } N, \text{ i.e., } I_0 \cup I_1 \cup F = N, \\ I_0, I_1 \text{ and } F \text{ are disjoint with each other} \end{array} \right\}.$$

Obviously,  $F$  is uniquely determined by  $I_0$  and  $I_1$  as  $F = N \setminus (I_0 \cup I_1)$  for each  $(I_0, I_1, F) \in \mathcal{S}$ . Hence,  $F$  in the triplet  $(I_0, I_1, F)$  is redundant, and we frequently omit  $F$  for the simplicity of notation. For each  $(I_0, I_1, F) \in \mathcal{S}$ , we consider a subproblem of BQOP (2)

$$\begin{aligned} \text{BQOP}(I_0, I_1) : \zeta(I_0, I_1) &= \min \left\{ \mathbf{x}^T \mathbf{B} \mathbf{x} : \begin{array}{l} \mathbf{x} \in \{0, 1\}^n, \sum_{i=1}^n x_i = 92, \\ x_i = 0 \ (i \in I_0), \ x_j = 1 \ (j \in I_1) \end{array} \right\} \\ &= \min \left\{ \mathbf{y}^T \mathbf{B}(I_0, I_1) \mathbf{y} : \begin{array}{l} \mathbf{y} \in \{0, 1\}^F, \\ \sum_{i \in F} y_i = 92 - |I_1| \end{array} \right\} + \sum_{j \in I_1} \sum_{k \in I_1} B_{jk}, \end{aligned}$$

where

$$\begin{aligned} \mathbf{y} \in \mathbb{R}^F &\text{ denotes the subvector of } \mathbf{x} \text{ with elements } x_i \ (i \in F), \\ \mathbf{B}(I_0, I_1) &= \mathbf{B}_{FF} + 2 \times \text{diagonal matrix of } \left( \sum_{k \in I_1} \mathbf{B}_{kF} \right), \\ \mathbf{B}_{kF} &= \text{the column vector consisting of elements } B_{kj} \ (j \in F). \end{aligned}$$

To see the equivalent representation of  $\mathbf{B}(I_0, I_1)$  above, we note that each  $x_k$  ( $k \in F$ ) in  $\text{BQOP}(I_0, I_1)$  is a binary variable; hence  $x_j x_k = x_k^2$  if  $j \in I_1$  and  $k \in F$ . For example, if  $F = \{1, \dots, \ell\}$  and  $I_1 \cup I_0 = \{\ell + 1, \dots, n\}$ , then  $\mathbf{B}(I_0, I_1)$  is an  $\ell \times \ell$  matrix with elements  $B(I_0, I_1)_{ij}$  ( $i = 1, \dots, \ell, j = 1, \dots, \ell$ ) such that

$$B(I_0, I_1)_{ij} = \begin{cases} B_{ij} & \text{if } i \neq j, \\ B_{ii} + 2 \sum_{k \in I_1} B_{ki} & \text{if } i = j. \end{cases}$$

For computing an LB of  $\text{BQOP}(I_0, I_1)$  in the BB method, we applied the NB method to the Lag-DNN relaxation of  $\text{BQOP}(I_0, I_1)$  with  $\lambda = 10^8 / \|\mathbf{B}(I_0, I_1)\|$ .

## 4.2 Orbital branching

We discuss the orbital branching technique from [32, 35]. As mentioned in Section 1,  $\mathbf{B} = \mathbf{B}(\emptyset, \emptyset)$  satisfies the symmetry property (3). This property is partially shared by numerous  $\mathbf{B}(I_0, I_1)$  instances where  $((I_0, I_1, F) \in \mathcal{S})$ . Let  $(I_0, I_1, F) \in \mathcal{S}$  be fixed. Assume in general that

$$\mathbf{y}_\sigma^T \mathbf{B}(I_0, I_1) \mathbf{y}_\sigma = \mathbf{y}^T \mathbf{B}(I_0, I_1) \mathbf{y} \text{ for every } \mathbf{y} \in \{0, 1\}^{|F|} \text{ and } \sigma \in \mathcal{G}(I_0, I_1) \quad (9)$$

holds, where  $\mathcal{G}(I_0, I_1)$  is a group of permutations of  $F$ . Let  $\omega(i) = \{j \in F : j = \sigma_i \text{ for some } \sigma \in \mathcal{G}(I_0, I_1)\}$  for every  $i \in F$ , and  $\mathcal{O}(I_0, I_1) = \{\omega(i) : i \in F\}$ . Each  $o \in \mathcal{O}(I_0, I_1)$

is called an *orbit* of the group  $\mathcal{G}(I_0, I_1)$ . Let  $\min(o)$  denote the minimum index of orbit  $o$ , which serves as a representative for  $o$ . Then we know that all  $\text{BQOP}(I_0, I_1 \cup \{j\})$  ( $j \in o$ ) are equivalent in the sense that they share a common optimal value  $\zeta(I_0, I_1 \cup \{\min(o)\})$ . Therefore, we can branch  $\text{BQOP}(I_0, I_1)$  to two sub BQOPs,  $\text{BQOP}(I_0 \cup o, I_1)$  and  $\text{BQOP}(I_0, I_1 \cup \{\min(o)\})$ .

In general,  $\mathcal{O}(I_0, I_1)$  consists of multiple orbits. Selecting an appropriate  $o$  from  $\mathcal{O}(I_0, I_1)$  for branching of  $\text{BQOP}(I_0, I_1)$  to  $\text{BQOP}(I_0 \cup o, I_1)$  and  $\text{BQOP}(I_0, I_1 \cup \{\min(o)\})$  is an important issue to design an efficient branch and bound method. In our numerical experiment presented in Section 4.4, an orbit  $o$  is chosen from  $\mathcal{O}(I_0, I_1)$  according to the average objective value of  $\text{BQOP}(I_0, I_1 \cup \min(o))$  over all feasible solutions, so that the chosen orbit,  $o^*$ , attains the largest value. Then, we apply the branching of  $\text{BQOP}(I_0, I_1)$  to two subproblems  $\text{BQOP}(I_0 \cup o^*, I_1)$  and  $\text{BQOP}(I_0, I_1 \cup \{\min(o^*)\})$ . Here the average objective value is computed as  $\mathbf{x}^T \mathbf{B} \mathbf{x}$  with  $x_i = 0$  ( $i \in I_0$ ),  $x_j = 1$  ( $j \in I_1$ ) and  $x_k = (92 - |I_1|)/|F|$  ( $k \in F$ ).

$\mathcal{G}(\emptyset, \emptyset) = \mathcal{G}$  has the single orbit  $o = N = \{1, \dots, n\}$ . We branch  $\text{BQOP}(\emptyset, \emptyset)$  into two subproblems  $\text{BQOP}(N, \emptyset)$  and  $\text{BQOP}(\emptyset, \{1\})$ . Obviously, the former  $\text{BQOP}(N, \emptyset)$  is infeasible. Table 1 summarizes the branching of the node  $\text{BQOP}(\emptyset, \{1\})$  to  $\text{BQOP}(\{2, 16, 17, 241\}, \{1\})$  and  $\text{BQOP}(\emptyset, \{1, 2\})$ , where orbit  $\{2, 16, 17, 241\}$  is chosen from  $\mathcal{O}(\emptyset, \{1\})$ .

| Orbit number | Orbit                         | The size of orbit | The average objective value of $\text{BQOP}(\emptyset, \{1, \min(o)\})$ |
|--------------|-------------------------------|-------------------|---|
| 1            | 2 16 17 241                   | 4                 | 52655297.0  |
| 2            | 18 32 242 256                 | 4                 | 52567852.0  |
| 3            | 3 15 33 225                   | 4                 | 52524130.0  |
| 4            | 19 31 34 48 226 240 243 255   | 8                 | 52515385.0  |
| 5            | 35 47 227 239                 | 4                 | 52502268.0  |
|              | ...                           |                   | ...   |
| 30           | 87 91 102 108 166 172 183 187 | 8                 | 52483274.0  |
| 31           | 9 129                         | 2                 | 52483139.0  |
| 32           | 72 74 117 125 149 157 200 202 | 8                 | 52483097.0  |
| 33           | 25 130 144 249                | 4                 | 52483097.0  |
|              | ...                           |                   | ...   |
| 43           | 121 136 138 153               | 4                 | 52481955.0  |
| 44           | 137                           | 1                 | 52481773.0  |

Table 1: A summary of branching of  $\text{BQOP}(I_0, I_1)$  with  $I_0 = \emptyset$ ,  $I_1 = \{1\}$  and  $F = \{2, 3, \dots, 256\}$  to  $\text{BQOP}(\{2, 16, 17, 241\}, \{1\})$  and  $\text{BQOP}(\emptyset, \{1, 2\})$ . Here  $F = \{2, 3, \dots, 256\}$  is partitioned into 44 orbits, which consist of 21 orbits with size 8, 21 orbits with size 4, 1 orbit with size 2 and 1 orbit with size 1. The 44 orbits are listed according to the decreasing order of the average objective value of  $\text{BQOP}(\emptyset, \{1, \min(o)\})$  over all feasible solutions.

In addition to the branching rule mentioned above, we employ the simple breadth first search; the method to search the enumeration tree is not relevant to the computational efficiency since the incumbent objective value is fixed to the target LB  $\hat{\zeta}$  and any upper bounding procedure is not applied. At the initial (0th) iteration, we take  $\text{BQOP}(I_0, I_1)$  with  $I_0 = \emptyset$  and  $I_1 = \{1\}$  as the active root node. Suppose that at the start of the  $k$ th iteration with  $k \geq 0$ , all active nodes located at depth  $k$  of the enumeration tree have already been generated. The  $k$ th iteration consists of two phases. First, we compute LBs of all active nodes to determine whether they remain active by applying the NB method. Second, we apply the orbital branching to the resulting active nodes, which are then located at depth

$(k + 1)$  of the enumeration tree, for the  $(k + 1)$ th iteration. At each node  $\text{BQOP}(I_0, I_1)$  of the enumeration tree, the NB method generates a sequence of intervals  $[a_p, b_p]$  ( $p = 1, 2, \dots$ ) satisfying a monotonicity property: (1)  $a_p$  converges monotonically to an LB  $\nu$  of  $\text{BQOP}(I_0, I_1)$  from below, and (2)  $b_p$  converges monotonically to  $\nu$  from above. Thus, if  $\hat{\zeta} \leq a_q$  holds for some  $q$ , we know that the LB  $\nu$  to which the interval  $[a_p, b_p]$  converges is not smaller than  $\hat{\zeta}$ , and  $\text{BQOP}(I_0, I_1)$  can be pruned. On the other hand, if  $b_q < \hat{\zeta}$  holds for some  $q$ , we know the LB  $\nu$  of  $\text{BQOP}(I_0, I_1)$  is smaller than  $\hat{\zeta}$ ; hence the iteration can be stopped and branching to  $\text{BQOP}(I_0, I_1)$  can be applied. Therefore, the above properties (1) and (2) of the NB method work very effectively to increase the computational efficiency of the BB method. See Figure 3.

### 4.3 Estimating the total number of nodes generated by the BB method

All the computations for numerical results reported in this section and the next two sections were performed using MATLAB 2022a on a Mac Studio with Apple M1 Ultra CPU, 20 cores and 128 GB memory. For the parallel computation, we solved Lag-DNN relaxations of 20 subproblems  $\text{BQOP}(I_0, I_1)$  in parallel by the NB method with the ‘parfor’ loop of MATLAB.

| target LB     |       | no. of nodes        |                     |                     | exec. timed (day) |                     |                     |
|---------------|-------|---------------------|---------------------|---------------------|-------------------|---------------------|---------------------|
| $\hat{\zeta}$ | gap   | min                 | mean                | max                 | min               | mean                | max                 |
| 44,100,000    | 1.46% | 22,175              | 27,278              | 29,692              | 0.9               | 1.1                 | 1.2                 |
| 44,120,000    | 1.43% | 53,625              | 72,574              | 91,944              | 2.1               | 2.8                 | 3.6                 |
| 44,130,000    | 1.41% | 64,084              | 133,417             | 275,264             | 2.5               | 5.2                 | 10.7                |
| 44,150,000    | 1.36% | 241,827             | 293,696             | 339,245             | 9.4               | 11.5                | 13.2                |
| 44,200,000    | 1.25% | 827,791             | 1,983,516           | 2,891,498           | 32.3              | 77.4                | 112.8               |
| 44,300,000    | 1.03% | $5.4 \cdot 10^7$    | $3.7 \cdot 10^8$    | $8.1 \cdot 10^8$    | $2.1 \cdot 10^3$  | $1.4 \cdot 10^4$    | $3.1 \cdot 10^4$    |
| 44,500,000    | 0.58% | $1.3 \cdot 10^{11}$ | $5.5 \cdot 10^{12}$ | $2.6 \cdot 10^{13}$ | $5.1 \cdot 10^6$  | $2.2 \cdot 10^8$    | $1.0 \cdot 10^9$    |
| 44,759,294    | 0.00% | $1.2 \cdot 10^{14}$ | $6.7 \cdot 10^{16}$ | $3.3 \cdot 10^{17}$ | $4.6 \cdot 10^9$  | $2.6 \cdot 10^{12}$ | $1.3 \cdot 10^{13}$ |

Table 2: Estimation of the work of the BB method described in Sections 4.1 and 4.2. For each target LB  $\hat{\zeta}$ , we applied 5 different random sampling of  $s_k$  nodes from  $\bar{t}_k$  active nodes at the depth  $k$  with  $k \geq \ell$  for the next depth  $k + 1$ . Here min, mean and max denote the minimum, the mean and the maximum of those 5 estimations of the number of nodes in the enumeration tree to generate and the execution time (day), respectively. A Lag-DNN subproblem at each node was solved in about  $30 \sim 150$  seconds.

To choose a reasonable target LB  $\hat{\zeta}$  which can be attained by the BB method, we performed preliminary numerical experiments to estimate the computational work. Given a target LB  $\hat{\zeta}$ , we construct an enumeration tree by the breadth first search as long as the number  $t_k$  of nodes at the depth  $k$  of the tree is smaller than 1000. Suppose that  $t_0, t_1, \dots, t_{\ell-1} < 1000 \leq t_\ell$ ; hence the full enumeration tree has been constructed up to the depth  $\ell$  by the BB method. We start sampling at the depth  $\ell$  and construct a random subtree to estimate the total number of nodes in the full enumeration tree. Let  $\bar{t}_\ell = t_\ell$ . At each depth  $k \geq \ell$ , we choose  $s_k$  nodes randomly from  $\bar{t}_k$  active nodes for the next depth  $(k + 1)$ , where

$$s_k = \begin{cases} 100 & \text{if } \bar{t}_k \geq 500, \\ \bar{t}_k & \text{otherwise.} \end{cases}$$

Then, we apply the lower bounding procedure using the NB method to the selected  $s_k$  nodes and the branching procedure to the resulting  $r_k$  active nodes to generate a subset of the nodes in the full enumeration tree at the depth  $(k + 1)$ . Next, we let  $\bar{t}_{k+1} = 2r_k$ , which is the cardinality of the subset (the number of nodes in the subset) as each active node is branched into two child nodes. We may regard  $2r_k/s_k = \bar{t}_{k+1}/s_k$  as the increasing rate of the nodes from the depth  $k$  to the depth  $k + 1$ , and the total number of nodes in the full enumeration tree is estimated by

$$\sum_{k=1}^{\ell} t_k + \sum_{k>\ell} \hat{t}_k, \text{ where } \hat{t}_\ell = t_\ell, \hat{t}_{k+1} = (2r_k/s_k)\hat{t}_k \text{ (} k \geq \ell \text{)}. \quad (10)$$

We continue this process till  $r_k$  attains 0. Table 2 shows the estimation of computational work (the number of nodes to generate and the execution time) for 8 cases  $\hat{\zeta} = 44,100,00, \dots, 44,759,294$ . In spite of the simplicity of this unrefined method, it provides useful information on whether a given target LB can be attained by the BB method on the computer used.

#### 4.4 Numerical results

We see from Table 2 that the cases with the target LB  $\hat{\zeta} = 44,759,294, 44,500,000$  and  $44,300,000$  are very challenging. The case  $\hat{\zeta} = 44,200,000$  could be processed but might take more than a few months. Table 3 shows numerical results for the other 4 cases with  $\hat{\zeta} = 44,100,000, 44,120,000, 44,130,000$  and  $44,150,000$ . We observe that the estimation of the number of nodes and execution time described in the previous section are useful.

| target LB     |       | no. of nodes              |                              | exec. time (day)          |                           |
|---------------|-------|---------------------------|------------------------------|---------------------------|---------------------------|
| $\hat{\zeta}$ | gap   | estimation (min,mean,max) | estimation (min,mean,max)    | estimation (min,mean,max) | estimation (min,mean,max) |
| 44,100,000    | 1.46% | 23,510                    | (22,175, 27,278, 29,692)     | 1.0                       | (0.9, 1.1, 1.2)           |
| 44,120,000    | 1.43% | 63,554                    | (53,625, 72,574, 91,944)     | 2.5                       | (2.1, 2.5, 3.6)           |
| 44,130,000    | 1.41% | 102,310                   | (64,084, 133,417, 275,264)   | 4.1                       | (2.5, 5.2, 10.7)          |
| 44,150,000    | 1.36% | 277,304                   | (241,827, 293,696, 339, 245) | 10.7                      | (9.4, 11.5, 13.2)         |

Table 3: Numerical results on the BB method described in Sections 4.1 and 4.2. The 3 numbers in the parenthesis  $(\cdot, \cdot, \cdot)$  denote the minimum, mean and maximum estimation from Table 2, respectively.

Figure 2 (A) displays the change in the number of nodes as the depth  $k$  increases, and Figure 2 (B) the change in the number of nodes with size 2 orbit. All other nodes are of the trivial single orbit  $N$ , except the root node having size 256 orbit as shown in Section 2.2 and the depth 1 node having sizes 1 through 8 orbit as observed in Table 4.2.

#### 4.5 Improving the BB method using isomorphism pruning

Through numerical results reported in Section 4.4, we found that even with the orbital branching, multiple subproblems appeared in the enumeration tree turned out to be isomorphic (equivalent) to each other. Here, two subproblems  $\text{BQOP}(I_0, I_1)$  and  $\text{BQOP}(I'_0, I'_1)$

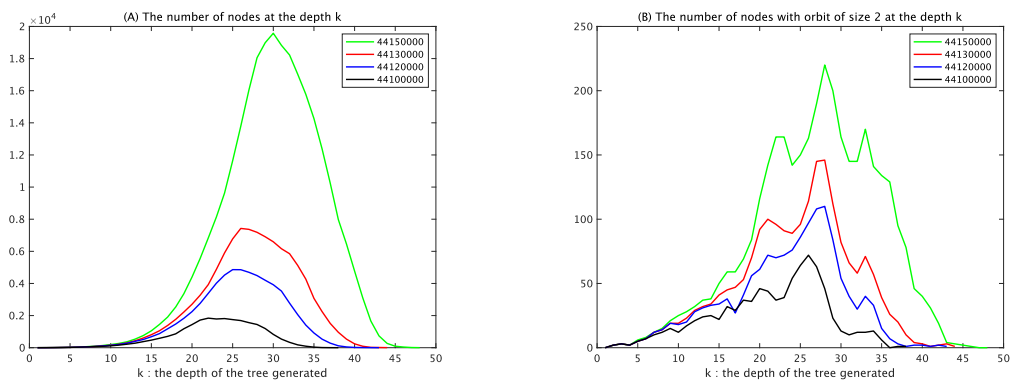


Figure 2: (A) The number of nodes of the enumeration tree at the depth  $k$ . (B) The number of nodes of the enumeration tree with size 2 orbit at the depth  $k$ .

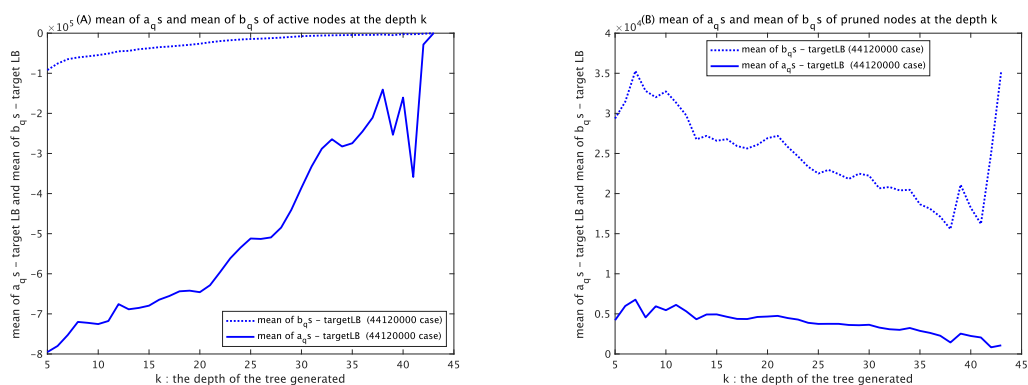


Figure 3: The mean of  $a_q$  (the blue solid line) and  $b_q$  (the blue dotted line) when the NB terminated at iteration  $q$  as  $b_q < \hat{\zeta} = 44,120,000$  (*i.e.*, active node) — Case (A) or at iteration  $q$  as  $\hat{\zeta} = 44,120,000 \leq a_q$  (*i.e.*, pruned node) — Case (B).

are called *isomorphic* if

$$|I_0| = |I'_0|, |I_1| = |I'_1|, \sum_{j \in I_1} \sum_{k \in I_1} B_{jk} = \sum_{j \in I'_1} \sum_{k \in I'_1} B_{jk}, \text{ and } \mathbf{B}(I'_0, I'_1) = \mathbf{P}^T \mathbf{B}(I_0, I_1) \mathbf{P}$$

for some permutation matrix  $\mathbf{P}$ . (11)

The isomorphic subproblems,  $\text{BQOP}(I_0, I_1)$  and  $\text{BQOP}(I'_0, I'_1)$ , share not only a common optimal value, but also a common LB, which is obtained as an optimal value of their Lag-DNN relaxations. Therefore, one of them can be pruned even when both of them are active. This technique is called the isomorphism pruning (see for example, [24] and the references therein). For a given pair of subproblems,  $\text{BQOP}(I_0, I_1)$  and  $\text{BQOP}(I'_0, I'_1)$ , checking (11) requires significantly less CPU time than computing their lower bounds. Moreover, various necessary conditions that are easy to implement can be used for verifying (11). Some of the conditions are, for instance,  $\sum_i [B(I'_0, I'_1)]_{ii} = \sum_i [B(I_0, I_1)]_{ii}$ ,  $\sum_{i,j} [B(I'_0, I'_1)]_{ij} = \sum_{i,j} [B(I_0, I_1)]_{ij}$ ,  $\max_i [B(I'_0, I'_1)]_{ii} = \max_i [B(I_0, I_1)]_{ii}$  and  $\min_{i,j} [B(I'_0, I'_1)]_{ij} = \min_{i,j} [B(I_0, I_1)]_{ij}$ . By applying those necessary conditions, the number of the candidates for pairs of subproblems  $\text{BQOP}(I_0, I_1)$  and  $\text{BQOP}(I'_0, I'_1)$  for which (11) is tested can be considerably reduced, before verifying (11).

We briefly outline our consistent implementation of the isomorphism pruning with the orbital branching. Suppose that we have a list of all generated nodes  $\{1, \dots, q\}$  of the depth  $1, \dots, k$  of the enumeration tree. The list includes all inactive (*i.e.* already pruned or branched) nodes  $1, \dots, p$  located at the depth  $1, \dots, k$  of the enumeration tree for some  $p < q$ , and all active (but not yet branched) nodes  $p + 1, \dots, q$  located at the depth  $k$ . We initially employ the orbital branching on active nodes  $p + 1, \dots, q$  and generate candidates for active nodes to which we will apply the lower bounding procedure, say  $N_a = \{q + 1, \dots, r\}$  for some  $r > q$ . Update the status of nodes  $p + 1, \dots, q$ , which have already undergone branching, from active to inactive. We then apply the isomorphism pruning to the entire node list  $\{1, \dots, r\}$  as follows:

Step 1: Let  $N_d = \emptyset$  (the set of node to be pruned from the enumeration tree by the isomorphism pruning).

Step 2: For every  $t = q + 1, \dots, r$ , if node  $t$  is isomorphic to some node  $s < t$ , then add  $t$  to  $N_d$ .

Step 3: Update the set  $N_a$  of active nodes by  $N_a \setminus N_d$ .

Now we are ready to apply the lower bounding procedure to the node set  $N_a$ . To simplify the explanation, we have assumed that we maintain the list of all generated nodes. However, only a subset of them is required at Step 2 above. For example, let  $f_1^{\min}$  denote the minimum of the numbers of variables fixed to 1 over the node set  $N_a = \{q + 1, \dots, r\}$ . Then, any node  $s \in \{1, \dots, q\}$  that has fewer than  $f_1^{\min}$  variables fixed to 1 is irrelevant at Step 2, as well as for future applications of isomorphism pruning, allowing us to eliminate  $s$  from the node set  $\{1, \dots, q\}$ .

Table 4 shows numerical results on the improved BB method in comparison to the original BB method whose numerical results have been reported in Section 4.4. We observe that the total number of nodes generated in the **improved BB** method is less than half of the one in the original BB method in all target LB cases, and that a larger target LB 44,200,000 (1.25% gap) is newly computed.



| target LB     |       | no. of nodes     |             | exec. time (day) |             |
|---------------|-------|------------------|-------------|------------------|-------------|
| $\hat{\zeta}$ | gap   | improved BB      | original BB | improved BB      | original BB |
| 44,100,000    | 1.46% | <b>11,594</b>    | 23,5100     | <b>0.6</b>       | 1.0         |
| 44,120,000    | 1.43% | <b>29,050</b>    | 63,554      | <b>1.2</b>       | 2.5         |
| 44,130,000    | 1.41% | <b>43,904</b>    | 102,310     | <b>1.8</b>       | 4.1         |
| 44,150,000    | 1.36% | <b>109,284</b>   | 277,304     | <b>4.3</b>       | 10.7        |
| 44,200,000    | 1.25% | <b>1,077,353</b> | -           | <b>39.2</b>      | -           |

Table 4: Numerical results on the improved BB method in comparison to the original BB method.

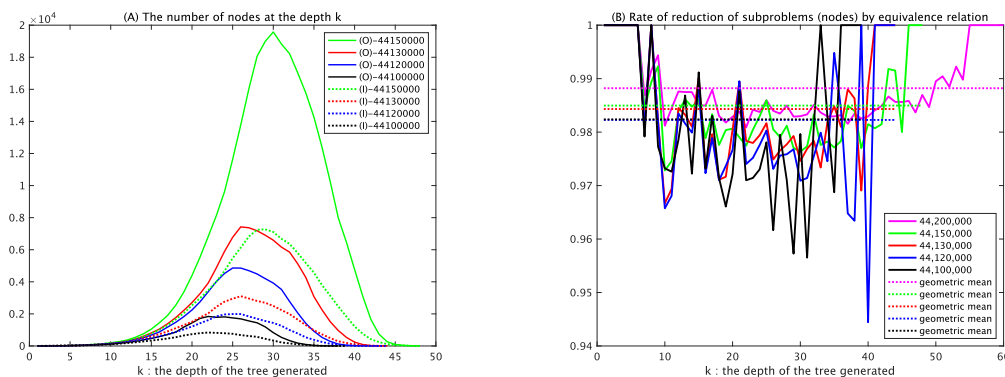


Figure 4: (A) Comparison of the numbers of nodes of the enumeration trees in the original BB method (O) and the improved BB method (I) at the depth  $k$  of their enumeration trees. (B) Reduction rate of subproblems at the depth  $k$  by the equivalence relation.

Figure 4 (A) compares the numbers of nodes at the depth  $k$  in the original and improved BB methods for the target LB = 44,100,000, 44,120,000, 44,130,000 and 44,150,000 cases. We can confirm that there exist significant differences between the numbers of nodes generated by them. Figure 4 (B) demonstrates the effectiveness of the isomorphism pruning technique at each depth  $k$  of the enumeration tree. Let  $v_k$  denote the number of active subproblems determined by the LB procedure at the depth  $k$ . Their  $2v_k$  subproblems are generated by the orbital branching. By applying the technique, we try to reduce the  $2v_k$  subproblems to which the LB procedure is applied at the depth  $k + 1$ . Suppose that some  $w_k$  nodes are pruned by the technique, where  $w_k$  could be 0. Figure 4 (B) shows the changes of  $(2v_k - w_k)/(2v_k)$  as  $k$  increases ( $k = 1, \dots, \ell$ ) and their geometric mean  $r = (\prod_{k=1}^{\ell} (2v_k - w_k)/(2v_k))^{1/\ell}$ , where  $\ell$  denotes the depth of the enumeration tree when the improved BB method terminated. In all target LB cases, we see that  $r \in [0.98, 0.99]$  in Figure 4 (B). It can be summarized that the technique reduces the number  $v_k$  of subproblems generated by the orbital branching to  $rv_k$  at the depth  $k$  on average, and the modified BB method can reduce the total number of nodes generated by the original BB method by the factor  $r^\ell$ .

From the discussions above, we can conclude that the technique proposed for pruning equivalent subproblems is indeed effective in accelerating the original BB method. We must say, however, that computing an LB with 1.1% gap remains very difficult since the technique would reduce the number of nodes generated by at most  $1/8 \in [0.98, 0.99]^{100}$ , where the improved BB method is assumed to terminate in the enumeration tree at the depth  $\ell = 100$ .

## 4.6 Remarks on the difficulty of BQOP (2)

By incorporating the isomorphism pruning in addition to the orbital branching, the improved BB method can entirely avoid the application of the lower bounding and branching procedures to more than one isomorphic subproblems of BQOP (2). It should be noted that these two techniques are useful for reducing the number of nodes in the enumeration tree that the BB method generates, but not for the lower bounding procedure itself. It is apparent that if we could employ a perfectly tight lower bounding procedure for any subproblem of BQOP (2), we could immediately determine whether the current UB attains the optimal value. However, this is purely ideal. We must acknowledge that even a high-quality lower bounding procedure is tight only for certain subproblems. Given this reality, we can say that solving the 256-dimensional BQOP (2) presents significant challenges, in comparison to BQOPs of similar size in the benchmark site [28, 41].

When a target LB is selected to be close to the unknown optimal value of BQOP (2), the difficulty in deciding whether to prune each subproblem heavily relies on its optimal value. Specifically, if the optimal value is close to the target LB, then the decision becomes more difficult. Conversely, if the optimal value is much larger than the target LB, then the decision becomes easier. The optimal value of the subproblem is determined by the minimum objective values over the feasible solutions of the subproblem. Therefore, we expect that the decision is more difficult (or easier) as BQOP (2) itself involves more (or fewer) feasible solutions with objective values close to the target LB, as the subproblem shares some of them. Thus, by sampling, we investigate the distribution of the objective values of feasible solutions of BQOP (2) in comparison to other BQOPs of similar size in

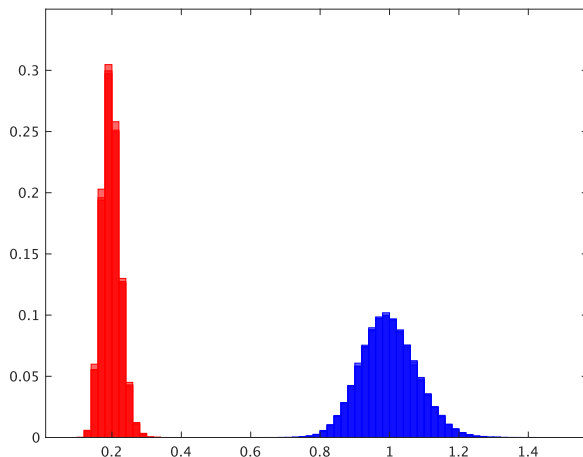


Figure 5: Distribution of the scaled objective values defined by (12). The horizontal axis represents the scaled objective value and the vertical axis the probability. The red histogram on the left depicts the distribution of the scaled objective values of 1,000,000 randomly chosen feasible solutions of BQOP (2). The blue histogram on the right depicts that of the 45 BQOPs (bqp250-1,...,bqp250-10, be200.3.1,...,be200.3.10, be200.8.1,...,be200.8.10,be250.1...,be250.10,gka1e,...,gka5e) with dimensions 200 or 250, where 1,000,000 feasible solutions are randomly sampled in each BQOP.

the benchmark site [41]. For the comparison, we apply the following scaling to objective values:

$$\text{the scaled objective value} = \frac{\text{the objective value} - \text{the optimal value of BQOP}}{|\text{the optimal value of BQOP}|}. \quad (12)$$

Figure 5 illustrates the distribution of the scaled objective values over 1,000,000 randomly chosen feasible solutions for BQOP (2) (the red histogram on the left) and that for 45 BQOPs from the benchmark site [41] (the blue histogram on the right). We can observe that the former is clearly smaller than the latter. This illustrates why BQOP (2) is notably more challenging compared to the benchmark BQOPs.

## 5 Concluding remarks

We have investigated the 256-dimensional BQOP with a single cardinality constraint, BQOP (2), which is converted from the largest unsolved QAP instance tai256c. The converted BQOP with dimension 256 is much simpler than the original QAP tai256c involving  $256 \times 256 =$

65536 binary variables, and its dimension 256 is not so large. While one might expect the converted BQOP to be notably easier to solve compared to the original QAP tai256c, our findings indicate that it still presents a significant challenge. The challenge primarily stems from the symmetry property (3) exhibited in the coefficient matrix  $\mathbf{B}$ , which is inherited from tai256c. For future development toward solving the BQOP, we need

- an efficient and much stronger lower bounding procedure than the DNN relaxation,
- additional techniques to enhance the exploitation of the symmetry property (3), and
- more powerful computer systems.

While we have focused on BQOP (2) converted from the QAP tai256c in this paper, it is straightforward to adapt the discussion of the paper to general BQOPs with a single cardinality constraint and general QUBOs which satisfy the symmetry property (3).

## Acknowledgements

The authors are grateful to Professor Koji Nakano for providing them with numerical results on DABS (Diverse Adaptive Bulk Search, a genetic algorithm-based search algorithm for solving QUBO [29]), which have been included in Section 4. They are also grateful to Tobias Achterberg for sharing the internal information of Gurobi and to Christopher Hojny for discussions about symmetry. The work of Sunyoung Kim was supported by NRF 2021-R1A2C1003810. The work for this article has been partially conducted within the Research Campus MODAL funded by the German Federal Ministry of Education and Research (BMBF grant numbers 05M14ZAM, 05M20ZBM).

## References

- [1] K. Anstreicher, N. Brixius, Goux J-P., Linderoth, and J. Solving large quadratic assignment problems on computational grids. *Math. Program.*, 91:563–588, 2002.
- [2] K. Anstreicher and H. Wolkowicz. On Lagrangian relaxation of quadratic matrix constraints. *SIAM J. Matrix Anal. Appl.*, 22(41-55), 2000.
- [3] N. Arima, S. Kim, M. Kojima, and K. C. Toh. Lagrangian-conic relaxations, Part I: A unified framework and its applications to quadratic optimization problems. *Pacific J. of Optim.*, 14(1):161–192, 2018.
- [4] N. Arima, S. Kim, M. Kojima, and K.C. Toh. A robust Lagrangian-DNN method for a class of quadratic optimization problems. *Comput. Optim. Appl.*, 66(3):453–479, 2017.
- [5] A. Beck and M. Teboulle. A fast iterative shrinkage-thresholding algorithm for linear inverse problems. *SIAM J. Imaging Sci.*, 2:183–202, 2009.
- [6] D. Brosch and E. de Klerk. Jordan symmetry reduction for conic optimization over the doubly nonnegative cone: theory and software. *Optim. Methods and Softw.*, page DOI: 10.1080/10556788.2021.2022146, 2022.

- [7] E. Burkard, R. E. Çela, S.E. Karisch, and F. Rendl. QAPLIB – a quadratic assignment problem library. *J. Global Optim.*, 10:391–403, 1997.
- [8] R.E. Burkard, E. Çela, S.E. Karisch, F. Rendl, M. Anjos, and P. Hahn. QAPLIB - A Quadratic Assignment Problem Library - Problem instances and solutions, <https://datashare.ed.ac.uk/handle/10283/4390>, 2022.
- [9] J. Clausen and M. Perregaard. Solving large quadratic assignment problems in parallel. *Comput. Optim. Appl.*, 8:111–127, 1997.
- [10] D. T. Connolly. An improved annealing scheme for the QAP. *Eur. J. Oper. Res.*, 46(93-100), 1990.
- [11] IBM Corporation. 2024. ILOG CPLEX Optimization Studio User’s Manual: <https://www.ibm.com/docs/es/icos/22.1.0>.
- [12] Etine de Klerk and R. Sotirov. Exploiting group symmetry in semidefinite programming relaxations of the quadratic assignment problem. *Math. Program.*, 122:225–246, 2010.
- [13] Etine de Klerk and R. Sotirov. Improved semidefinite programming bounds for quadratic assignment problems with suitable symmetry. *Math. Program.*, 133:75–91, 2012.
- [14] M. Fischetti, M. Monaci, and D. Salvagnin. Three ideas for the quadratic assignment problem. *Oper. Res.*, 60(4):Published Online:1 Aug 2012, 2012.
- [15] L. M. Gambardella, E. D. Taillard, and M. Dorigo. Ant colonies for the QAP. Technical report idsia-4-97, IDSIA, Lugano, Switzerland, 1997.
- [16] P. C. Gilmore. Optimal and suboptimal algorithms for the quadratic assignment problem. *SIAM J. Appl. Math.*, 10:305–313, 1962.
- [17] A. D. Goncalves, A. A. Pessoa, L. M. de A. Drummond, C. Bentes, and R. Farias. Solving the quadratic assignment problem on heterogeneous environment (CPUs and GPUs) with the application of level 2 reformulation and linearization technique. Technical Report [arXiv:1510.02065v1](https://arxiv.org/abs/1510.02065), 2015.
- [18] LLC Gurobi Optimization. 2024. Gurobi Optimizer Reference Manual: <https://www.gurobi.com>.
- [19] N. Ito, S. Kim, M. Kojima, A. Takeda, and K.C. Toh. Equivalences and differences in conic relaxations of combinatorial quadratic optimization problems. *J. Global Optim.*, 72(4):619–653, 2018.
- [20] S. Ji, X. Zheng, and X Sun. An improved convex 0-1 quadratic program reformulation for quadratic knapsack problems. *Pacific J. of Optim.*, 8(1):75–87, 2012.
- [21] S. Kim, M. Kojima, and K. C. Toh. A Lagrangian-DNN relaxation: a fast method for computing tight lower bounds for a class of quadratic optimization problems. *Math. Program.*, 156:161–187, 2016.

- [22] S. Kim, M. Kojima, and K. C. Toh. A Newton-bracketing method for a simple conic optimization problem. *Optim. Methods and Softw.*, 36:371–388, 2021.
- [23] E. L. Lawler. The quadratic assignment problem. *Management Sci.*, 19:586–590, 1963.
- [24] F. Margot. Pruning by isomorphism in branch-and-cut. *Mathematical Programming*, 94:71–90, 2002.
- [25] B. D. McKay. Nauty users guide (version 2:4). Technical report, Dept. Comp. Sci., Australian National University, 2010.
- [26] H. Mittelmann. Benchmarks for optimization software. <http://plato.asu.edu/bench.html>, 2012. Accessed: Nov 2023.
- [27] H. Mittelmann. Improved QAPLIB lower bounds using BBCPOP and Newton-Bracket, [https://plato.asu.edu/ftp/qaplib\\_bounds.html](https://plato.asu.edu/ftp/qaplib_bounds.html), December 2023.
- [28] H. Mittelmann. Nonconvex QUBO-QPLIB benchmark, <https://plato.asu.edu/ftp/qubo.html>, September 2023.
- [29] K. Nakano, D. Takafuji, Y. Ito, T. Yazane, S. Yano, J. an, R. Katsuki, and R. Mori. Diverse adaptive bulk search: a framework for solving qubo problems on multiple gpus. In *Proc. of 2023 IEEE International Parallel and Distributed Processing Symposium Workshops (IPDPSW)*, pages 314–325, May, 2023.
- [30] O Nissofolk, R. Pörn, and T. Westerlund. Testing a non-diagonal convex reformulation technique for 0-1 quadratic programs. Presentation at ESXAP 26, Slides, <https://blogs.abo.fi/ose/files/2017/02/Westerlund-ESCAPE26.pdf>, June 2016.
- [31] O Nissofolk, R. Pörn, and T. Westerlund. Testing the non-diagonal quadratic convex reformulation technique. In *Proceedings of the 26th European Symposium on Computer Aided Process Engineering-ESCAPE 26*, pages 331–336. Elsevier, June 2016.
- [32] J. Ostrowski, J. Linderoth, Rossi F., and S. Smriglio. Orbital branching. *Math. Program.*, 126:147–178, 2011.
- [33] P. M. Pardalos, K. G. Ramakrishnan, M. G. C. Resende, and Y. Li. Implementation of a variance reduction-based lower bound in a branch-and-bound algorithm for the quadratic assignment problem. *SIAM J. Optim.*, 7:281–294, 1997.
- [34] F.N. Permenter and P. A. Parrilo. Dimension reduction for semidefinite programs via jordan algebras. *Math. Program.*, 181:51–84, 2020.
- [35] M. E. Pfetsch and Rehn T. A computational comparison of symmetry handling methods for mixed integer programs. *Math. Program. Comput.*, 11:37–93, 2019.
- [36] J. Povh and F. Rendl. Copositive and semidefinite relaxations of the quadratic assignment problem. *Discrete Optim.*, 6:231–241, 2009.
- [37] C. Roucairol. A parallel branch and bound algorithm for the quadratic assignment problem. *Discret. Appl. Math.*, 18:211–255, 1987.

- [38] Hanif D Sherali and Warren P Adams. *A reformulation-linearization technique for solving discrete and continuous nonconvex problems*. Springer Science & Business Media, 2013.
- [39] J. Skorin-Kapov. Tabu search applied to the quadratic assignment problem. *ORSA J. Comput.*, 2:33–45, 1990.
- [40] E. Tailard. Robust taboo search for the quadratic assignment problem. *Parallel Comput.*, 17:443–455, 1991.
- [41] A. Wiegele. Biq mac library. <http://www.biqmac.uni-klu.ac.at/biqmaclib.html>, 2007.
- [42] Q. Zhao, S.E. Karisch, F. Rendl, and H. Wolkowicz. Semidefinite programming relaxations for the quadratic assignment problem. *J. Comb. Optim.*, 2(71-109), 1998.